

(p, t) Reaction on Even-Even $N=Z$ Nuclei in the $2s1d$ Shell*

R. A. Paddock†

Cyclotron Laboratory and Physics Department, Michigan State University, East Lansing, Michigan 48823

(Received 21 June 1971)

The (p, t) reaction on the even-even $N=Z$ nuclei in the $2s1d$ shell has been used to study the energy levels of ^{18}Ne , ^{22}Mg , ^{26}Si , ^{30}S , ^{34}Ar , and ^{38}Ca . The energies of the excited states observed are reported along with spin and parity assignments when possible. Two-nucleon-transfer distorted-wave calculations were carried out. Comparisons are made with the shapes of the experimental angular distributions. It is found that the calculated shapes are primarily dependent upon the L transfer and the optical-model parameters. The magnitudes of the calculated cross sections are found to depend strongly not only on the optical-model parameters, but also the bound-state parameters and the configuration mixing in the initial and final nuclear wave functions.

I. INTRODUCTION

The (p, t) two-nucleon-transfer reaction has been studied for even-even $N=Z$ targets in the $2s1d$ shell. In particular, the targets were ^{20}Ne , ^{24}Mg , ^{28}Si , ^{32}S , ^{36}Ar , and ^{40}Ca , which all have $J^\pi=0^+$ ground states. These (p, t) reactions reach states in nuclei which are two nucleons away from stability. The only other way of reaching the same nuclei by a two-body final-state reaction is the $(^3\text{He}, n)$ reaction. Until recently these nuclei have not been studied to any great extent although the (p, t) reaction has been used extensively to study nuclei in the light-mass region¹⁻³ and in the medium-to-heavy-mass region.⁴⁻⁸ These studies have shown that the shapes of the angular distributions are characteristic of the L transfer.

We denote the reaction by

$$A(p, t)B,$$

and the transferred quantum numbers by L , S , J , and T . Since the targets are all $J_A=0$, $T_A=0$, and since $T=1$ is a requirement of the (p, t) reaction, it follows that $J_B=J$ and $T_B=1$. The two neutrons bound in the triton are mostly ($\sim 95\%$)⁹ in a state of relative spatial symmetry which requires that $S=0$. This leads to $J_B=L$ as an approximate restriction. If it is further assumed that the neutrons in the triton are in a relative s state, then the parity change is restricted to $\Delta\pi=(-1)^L$. These restrictions make the spin-parity assignments to the final nuclear states quite unambiguous once the L transfer has been established.

II. THEORY

The conventional distorted-wave method for di-

rect reactions such as set forth by Satchler¹⁰ was used to calculate the shapes of the angular distributions. The details of the reaction mechanism are calculated by a spin-dependent distorted-wave computer code in a zero-range approximation. Glendenning¹¹ developed the form factor needed in this calculation by using harmonic-oscillator wave functions for the two bound neutrons and a Gaussian wave function for the triton. It has been shown by Drisko and Rybicki¹² that the use of finite-well wave functions alters considerably the predicted cross section. We choose to follow the finite-well wave-function approach as expressed in detail in a paper by Jaffe and Gerace.¹³

The bound-state wave functions of the two neutrons are taken to be those of a particle bound in a well of the form

$$U(r) = -V_0 f(r) + \left(\frac{\hbar}{m_\pi c}\right)^2 V_s \frac{1}{r} \frac{d}{dr} f(r) \vec{l} \cdot \vec{\sigma},$$

where $f(r)$ is taken to be the standard Woods-Saxon shape with $r_0=1.25$ fm and $a=0.65$ fm as suggested by Bayman and Hintz,⁶ and V_s was taken as 6 MeV, which is typical of single-nucleon spin-orbit strengths. The real well depth was adjusted so that the individual neutrons were bound by one-half the two-neutron separation energy as suggested in Refs. 6 and 12. These wave functions were expanded in terms of harmonic-oscillator wave functions with typically five to eight terms needed to fit the Woods-Saxon wave function to better than 2% out to twice the nuclear radius. The calculations of the individual form factors were carried out by the computer code TWOFRM (written by W. Gerace, Princeton University). The distorted-wave calculations were carried out with the code JULIE.¹⁴ The distorted waves were obtained from an optical-model po-

TABLE I. Optical-model parameters.

	V_0 (MeV)	W_0 (MeV)	W_D (MeV)	V_S (MeV)	r_0 (fm)	a (fm)	r'_0 (fm)	a' (fm)	r''_0 (fm)	a'' (fm)	r_{0C} (fm)	Ref.
Proton	42	0	8.5	7.5	1.18	0.7	1.04	0.7	1.18	0.7	1.2	15
Triton	168	17	0	0	1.16	0.752	1.498	0.817			1.25	16

tential of the form

$$U_{\text{OM}}(r) = V_C(r_{0C}) - V_0 f(r_0, a) - i \left(W_0 - 4a' W_D \frac{d}{dr} \right) f(r'_0, a') + \left(\frac{\hbar}{m_\pi c} \right)^2 V_S \frac{1}{r} \frac{d}{dr} f(r''_0, a'') \vec{1} \cdot \vec{\sigma},$$

where

$$f(r_0, a) = \left(1 + \exp \frac{r - r_0 A^{1/3}}{a} \right)^{-1}.$$

The first term is the Coulomb potential of a uniformly charged sphere of radius $r_{0C} A^{1/3}$. For spin- $\frac{1}{2}$ particles, $\vec{\sigma} = 2\vec{S}$. In order to be as consistent as possible among all six nuclei, a single set of proton and triton optical parameters was used throughout. These parameters are listed in Table I.^{15, 16} In both cases average geometries over the appropriate range of A were used. The well depths were varied over a small range in order to obtain the best average fit to the ground-state transitions.

III. EXPERIMENTAL PROCEDURES

A. Proton Beam

The Michigan State University sector-focused cyclotron was used to provide a beam of 40- to 45-MeV protons. The beam was energy-analyzed and spatially defined by two 45° bending magnets and three sets of slits. The beam resolution was calculated from measured magnetic fields and slit apertures to be about 40 keV. The details of this transport system have been discussed by MacKenzie *et al.*¹⁷

A 36-in.-diam evacuated scattering chamber was used. Both solid foil targets and gas-cell targets were employed. The detector telescope was mounted on a movable arm and, in the case of foil targets, a monitor counter was mounted on a relocatable stationary arm. The position of the movable arm was remotely adjustable with an accuracy and reproducibility of about 0.15°.

The beam from the chamber was stopped and collected in an external aluminum Faraday cup. The beam current was monitored, and the total charge collected was measured.

B. Targets

The ^{20}Ne target was a 3-in.-diam gas cell with $\frac{1}{2}$ -mil Kapton windows. The gas was natural neon, which is about 90.9% ^{20}Ne . The gas pressure was maintained at about 28 cm of Hg. A proton energy of 45.0 MeV was used.

The ^{24}Mg target was a self-supporting foil of magnesium metal enriched to 99.96% ^{24}Mg . This foil was obtained from Union Carbide at the Oak Ridge National Laboratory. It was reported to be 566 $\mu\text{g}/\text{cm}^2$ thick, and this thickness was used in normalizing the cross sections obtained. For this purpose the thickness was assumed to be accurate to $\pm 5\%$. 41.9-MeV protons were used.

The ^{28}Si target was a self-supporting foil of natural silicon metal (92.21% ^{28}Si). This foil was also obtained from Union Carbide. Its thickness was determined by measuring the energy loss of α particles from a natural source when they passed through the foil. The results were compared with range tables¹⁸ to determine the thickness. The thickness was found to be 687 $\mu\text{g}/\text{cm}^2$ and an accuracy of $\pm 5\%$ was assumed for normalization purposes. The proton energy was 42.1 MeV.

The ^{32}S target was a 5-in.-diam gas cell with $\frac{1}{2}$ -mil Kapton windows. The gas was natural H_2S ($\sim 95.0\%$ ^{32}S) at a pressure of about 21 cm of Hg. The beam energy was 39.9 MeV.

Two different ^{36}Ar targets were used. Both were 3-in. gas cells filled with argon gas enriched to

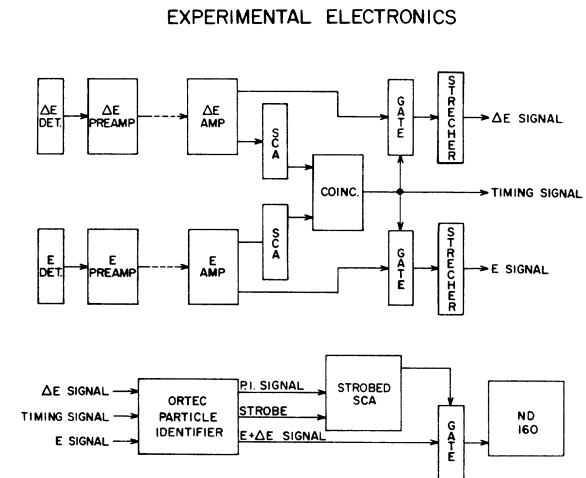


FIG. 1. Experimental electronics.

>99% ^{36}Ar . The first cell was a sealed cell, with $\frac{1}{2}$ -mil Havar windows and a pressure of 45.1 ± 1.0 cm of Hg, built by Kozub.¹⁹ The thick windows (10 mg/cm^2) caused some problems in triton energy resolution. The second cell had $\frac{1}{2}$ -mil Kapton windows ($\sim 1.7 \text{ mg/cm}^2$) and a pressure of 26 cm of Hg. Better resolution was obtained with this target and so it was used for energy-calibration purposes. It also served as a check on the actual gas pressure of the sealed cell, which was over a year old. Again 39.9-MeV protons were used.

The ^{40}Ca target was a self-supporting foil of natural calcium (96.97% ^{40}Ca). This foil was prepared by evaporating in vacuum calcium metal onto a tantalum backing. Upon cooling, the calcium foil was easily removed. The thickness was measured with α particles in the same way as described for the ^{28}Si target. Its thickness was found to be $863 \mu\text{g/cm}^2$ and an error of $\pm 4\%$ was assumed for normalization purposes. A thinner target ($\sim 690 \mu\text{g/cm}^2$) was used for some runs, but all the data were normalized to the first target. 40.1-MeV protons were used.

C. Detectors and Electronics

The detector telescope was made up of two silicon surface-barrier transmission mounted counters. The first counter was relatively thin and will be designated the ΔE counter. The second was thicker and will be called the E counter. The particular counters used depended upon the specific experiment. In the ^{36}Ar , ^{24}Mg , and ^{28}Si experiments, both triton and the ^3He data were taken. In order to allow the ^3He particles to reach the E counter, the ΔE counter was chosen to be somewhat thinner than in the other experiments.

The experiments involving foil targets required only one collimator in front of the detectors. These

collimators were made of 50 to 90 min tantalum located at 8 to 11 in. from the target. Both round apertures and oval apertures were used. The oval collimators were smaller in the horizontal direction in order to minimize kinematic broadening and yet increase the effective solid angle.

When gas-cell targets were used, two collimators were needed to define the volume of gas that was to be considered the target. The front collimator nearest the gas cell was a tall brass slit with a full width of about 125 mil. The back collimators were the same ones previously mentioned for foil targets and were located from 9 to $12\frac{1}{2}$ in. from the center of the cell. The front collimator was from 5 to $8\frac{1}{2}$ in. ahead of the back collimator.

The monitor counter which was used with foil targets consisted of a NaI crystal and a photomultiplier tube. It was held at a fixed angle and a single-channel analyzer (SCA) was set with its window about the elastically scattered proton peak. In this way the output of the SCA was proportional to the product of the beam current and the effective target thickness.

The experiment with the ^{36}Ar , ^{24}Mg , and ^{28}Si targets employed the ORTEC model No. 423 particle identifier which is based on the technique developed by Goulding *et al.*²⁰ The total energy spectrum, gated by the particle-identifier output, was analyzed and stored in a pulse-height analyzer. Figure 1 shows a block diagram of the electronics involved.

The experiments with ^{20}Ne and ^{40}Ca targets used a different method of particle identification also based on the differential energy loss. The signals from the ΔE and E counters were summed (called the Σ signal) at the detector telescope, and all three pulses (ΔE , E , and Σ) were passed through charge-sensitive preamplifiers and sent to the data-acquisition area. Figure 2 shows this summing circuit. Using an electronic setup similar to the previous method, a slow coincidence was required between the ΔE and E signals. These two signals then went to a dual analog-to-digital converter (ADC). An XDS Sigma-7 on-line computer and the data-acquisition computer code TOOTSIE²¹ were used to analyze the digital signals from the ADC. TOOTSIE displays, on a cathode-ray screen, ΔE versus Σ . Because of the difference in energy loss (ΔE signal) of particles of different charge and mass for the same energy (Σ signal), the different particles fall into bands on the two-dimensional plot. The code then allows gate lines to be introduced in the form of polynomial fits to designated points. These gate lines are then used to route the Σ signal to any of four 2048-channel spectra.

In the case of the ^{32}S experiment, two detector

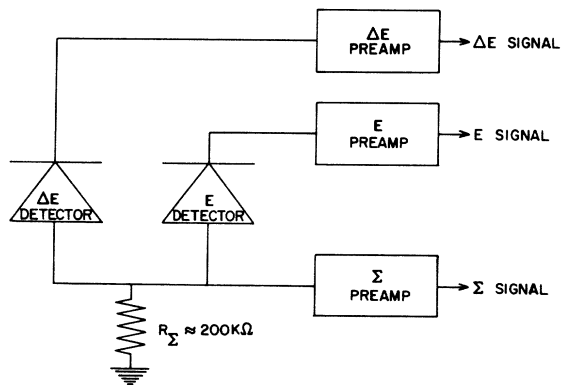


FIG. 2. Summing circuit.

telescopes, placed 10° apart on the scattering chamber arm, were used. The particle-identification system using the on-line computer was used. After the coincidence and linear gates the ΔE and Σ signals from the two telescopes were mixed and sent to the ADC, along with a routing signal taken from the coincidence modules.

D. Triton Energy Spectra

In the earlier experiments (Ar, Mg, and Si), the electronic limitation on the resolution was measured by introducing a pulser signal, through a

1- or 2-pF capacitor, into the preamps. It was found to be equivalent to 45 to 65 keV full width at half maximum (FWHM). In the later experiments when the total energy signal (Σ) was taken from the summing circuit at the detector telescope, electronic contributions were reduced to 30 to 40 keV FWHM.

The over-all experimental resolution varied with the particular target, counters, and electronic configuration. For the ^{20}Ne and ^{32}S cases the resolution was about 90 keV FWHM. The ^{24}Mg experiment had about 120 keV. The ^{28}Si case was

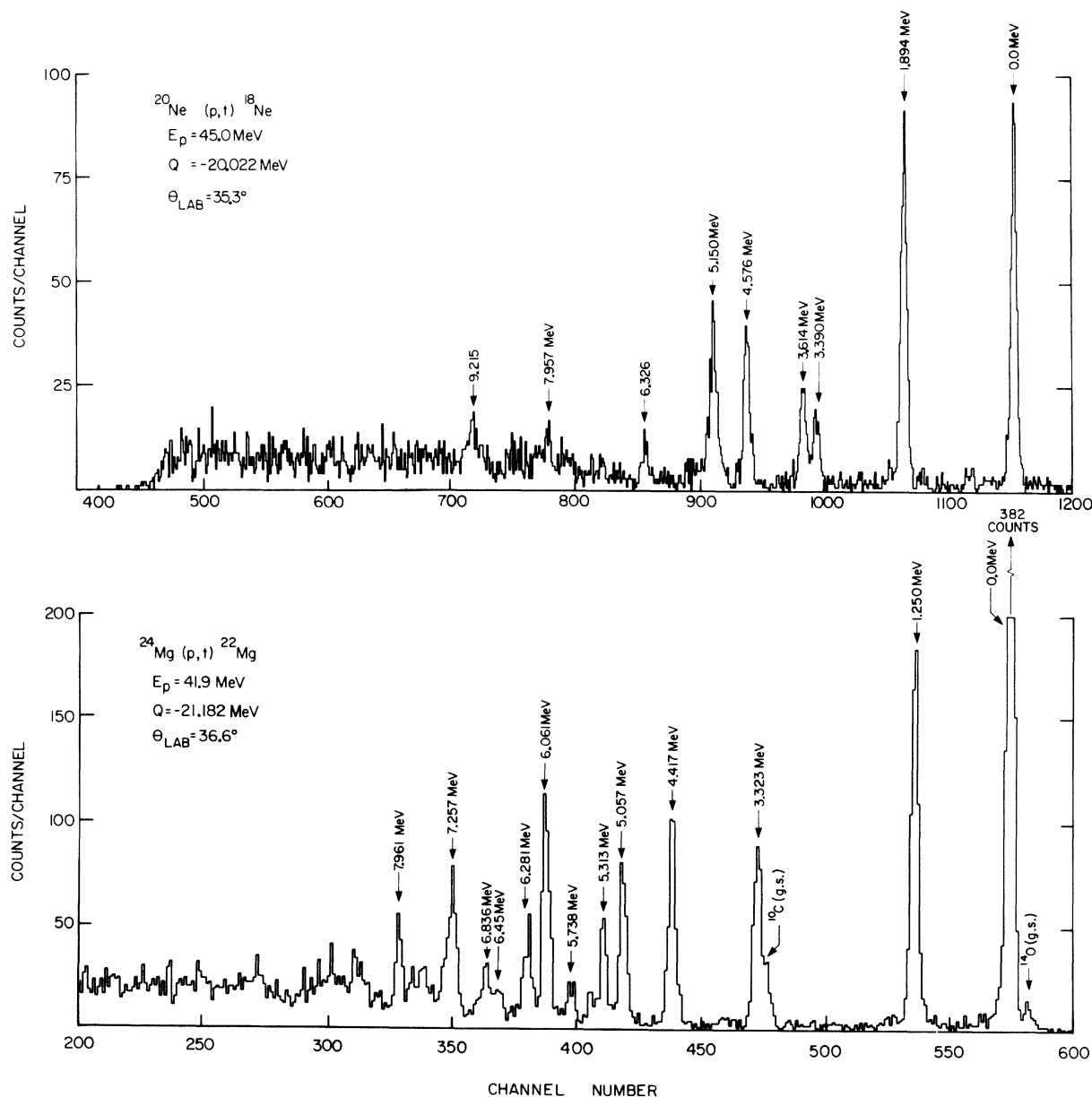


FIG. 3. Triton spectra from $^{20}\text{Ne}(p,t)^{18}\text{Ne}$ and $^{24}\text{Mg}(p,t)^{22}\text{Mg}$.

about 140 keV. The ^{36}Ar gas cell with the thick Havar windows gave 155 keV, while the cell with Kapton windows gave 100 keV. The ^{40}Ca experiment had about 60-keV over-all resolution. Figures 3-5 show sample triton energy spectra for each target.

IV. EXPERIMENTAL RESULTS

The excitation energies of the levels observed

by the (p, t) reaction are listed in Tables II through VII.²²⁻⁴⁹ Included are the J^π assignments for levels when the experimental angular distributions were distinctive enough to indicate L transfer. Also shown are the levels seen by other workers and their J^π assignments. Values in parentheses represent tentative assignments; double parentheses indicate that the assignment is extremely tentative. In order to limit these tables to a convenient size, only the more recent references are

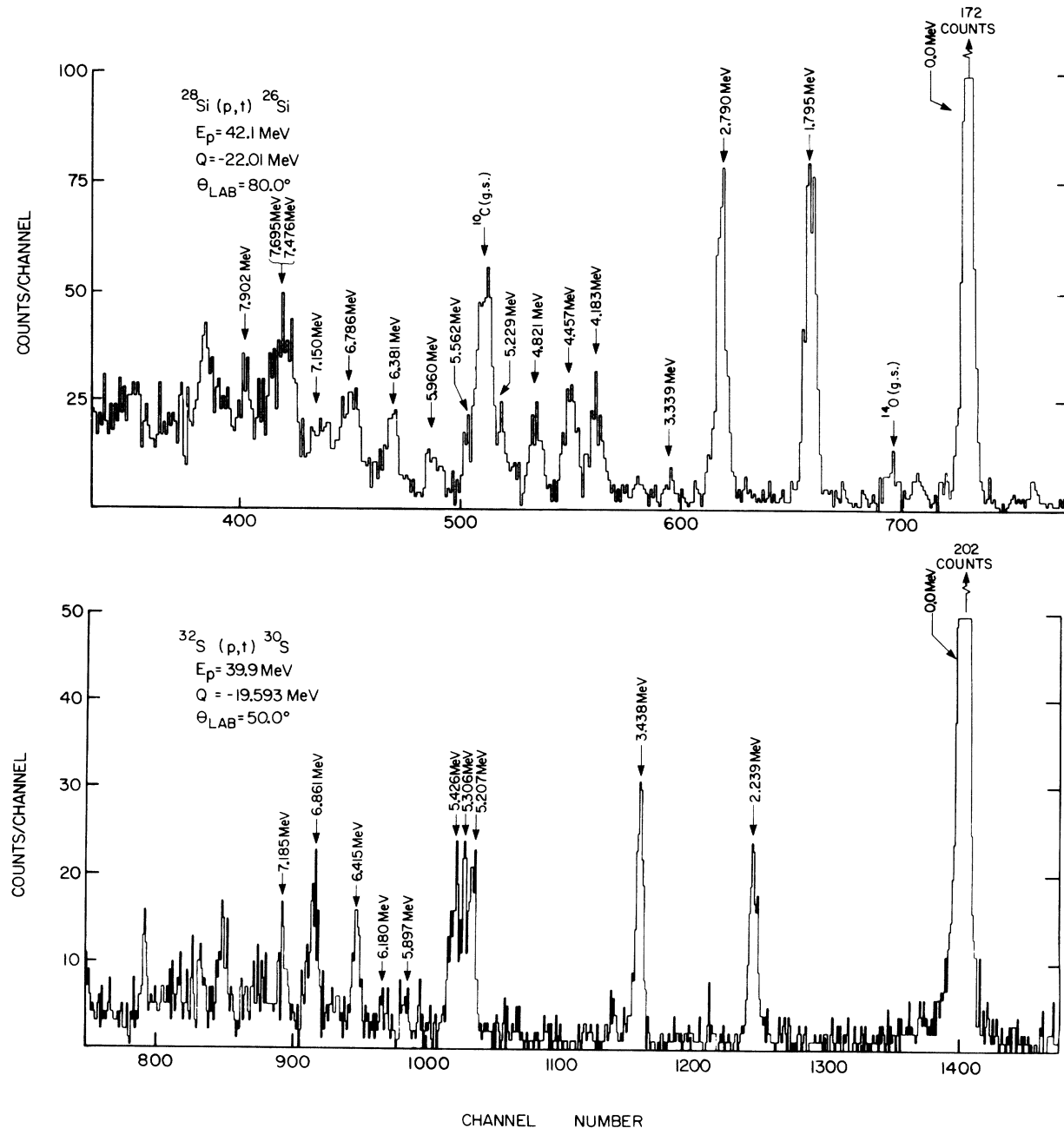


FIG. 4. Triton spectra from $^{28}\text{Si}(p,t)^{26}\text{Si}$ and $^{32}\text{S}(p,t)^{30}\text{S}$.

given. The excitation energy listed is usually taken from the reference with the smallest quoted error. Correspondence with levels seen in the present work is made whenever possible. This correspondence, of course, may not always be correct. All references are to (${}^3\text{He}, n$) or (${}^3\text{He}, n\gamma$) work unless followed by a superscript t , in which case the (p, t) reaction was used. The subscripts J , π , or E indicate that the spin, parity, or energy assignment was taken from that reference if it is not the only one. The mass excesses (M.E.) quoted are sometimes averages of several experiments taken from the compilations of Mattauch, Thiele, and Wapstra²² and Endt and Van der Leun.³⁴ Angular distributions were obtained for several of the more strongly excited levels. These levels are

indicated by an * next to the excitation energy in the tables. Because of background and resolution limitations and interference from impurities in the target, the other states were only observed or resolved at two to six different angles and so complete angular distributions were not obtained. The experimental over-all normalization uncertainty for the measured cross sections is about $\pm 10\%$ for the foil targets and about $\pm 5\%$ for the gas targets.

V. DISTORTED-WAVE ANALYSIS

A. Ground-State Transitions

Distorted-wave calculations were made for the six 0^+ -to- 0^+ ground-state transitions assuming the pickup of a pair of neutrons coupled to angular

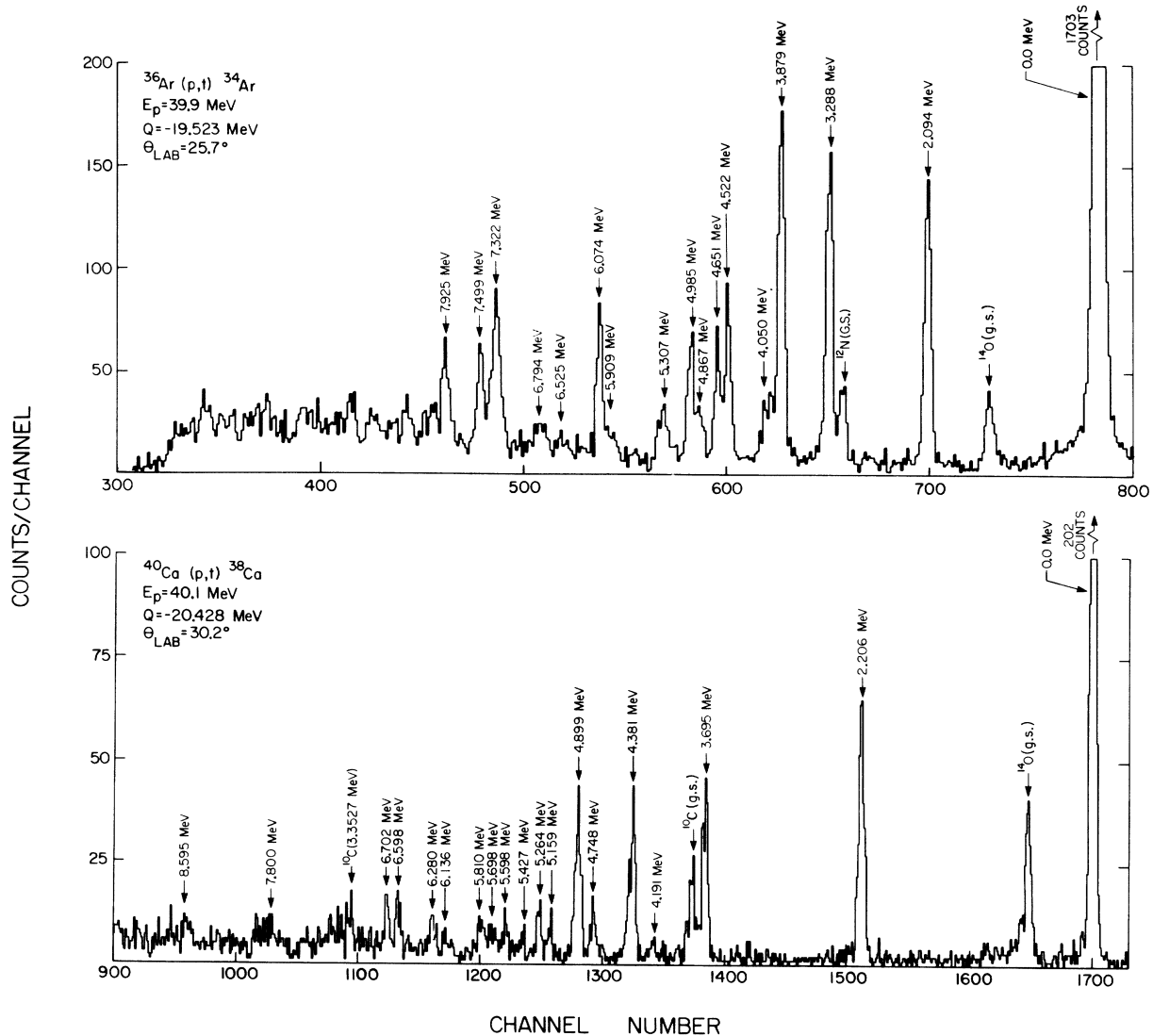


FIG. 5. Triton spectra from ${}^{36}\text{Ar}(p, t){}^{34}\text{Ar}$ and ${}^{40}\text{Ca}(p, t){}^{38}\text{Ca}$.

TABLE II. Energy levels of ^{18}Ne . See text for explanation of notation.

This work		Other work		
Energy (MeV)	J^π	Energy (MeV)	J^π	References
		M.E. = 5.3193 ± 0.0047		22
0.0*	0^+	0.0	0^+	$23^t, 24^t, 25, 26, 27_J, 28, 29^t$
$1.894^* \pm 0.010$	2^+	1.8873 ± 0.0002	2^+	$23^t, 25, 26, 27_{J\pi}, 29^t, 30_E, 31$
$3.390^* \pm 0.014$	(4^+)	3.3762 ± 0.0004	4^+	$23^t, 26, 29^t, 30_E, 32_{J\pi}$
$3.614^* \pm 0.013$	(0^+)	3.5763 ± 0.0020	(0)	$29^t, 30_{EJ}, 31$
		3.6164 ± 0.0006	2^+	$23^t, 26, 29_{EJ\pi}, 31, 32$
4.576*	$(1^-, 0^+)$	4.505 and 4.571 ± 0.015	0^+ and 1^-	$23^t, 26, 29^t, 33_{EJ\pi}$
$5.150^* \pm 0.014$		5.12		$29^t, 33$
$6.326^* \pm 0.018$				
7.957 ± 0.025				
$9.215^* \pm 0.020$				

momentum zero from the last shell in the simple j - j coupled shell-model picture. Each individual proton shell and neutron shell was assumed to be coupled to zero angular momentum.

The experimental cross sections should be proportional to the calculated cross sections if the proper wave functions, and thus parentage factors, are used, along with the proper distorted waves. Since the simple wave functions described above

are not adequate, the proportionality factor cannot be expected to be constant, and it is not. Figure 6 shows the data for the six 0^+ -to- 0^+ ground-state transitions along with the distorted-wave calculations based on these simplest of wave functions. The calculations have been multiplied by $K/5014$, where K was adjusted to give the best average fit to the first two maxima of the data.

Another method of calculating (p, t) angular dis-

TABLE III. Energy levels of ^{22}Mg . See text for explanation of notation.

This work		Other work		
Energy (MeV)	J^π	Energy (MeV)	J^π	References
M.E. = -0.4123 ± 0.0097		M.E. = -0.389 ± 0.011		$34^t, 35_E$
0.0*	0^+	0.0	0^+	36
$1.250^* \pm 0.008$	2^+	1.2450 ± 0.0006	2^+	$25_{J\pi}, 37^t, 38_E, 39, 40^t, 35$
$3.323^* \pm 0.021$	(4^+)	3.353 ± 0.045	(4^+)	$25_{J\pi}, 37^t_E, 39, 40^t$
$4.417^* \pm 0.027$	(2^+)	4.378 ± 0.035	(2^+)	$25_{J\pi}, 35_E, 37^t$
$5.057^* \pm 0.031$	(2^+)	5.032 ± 0.030	2^+	$25, 35_{EJ\pi}$
		5.130 ± 0.035		40
$5.313^* \pm 0.032$		5.286 ± 0.030	$(2^+, 3^-, 4^+)$	$25_{J\pi}, 35_E$
		5.433 ± 0.030	$(2^+, 3^-, 4^+)$	$25_{J\pi}, 35_E$
$5.738^* \pm 0.035$		5.699 ± 0.020	$((0^+))$	$25_{J\pi}, 35_E$
$6.061^* \pm 0.037$	0^+	5.945 ± 0.020	0^+	35
$6.281^* \pm 0.033$		6.263 ± 0.020		35
6.645 ± 0.044		6.573 ± 0.020		35
6.836 ± 0.044		6.770 ± 0.020		35
$7.257^* \pm 0.044$		7.201 ± 0.020		35
$7.961^* \pm 0.049$				

tributions using distorted waves is to treat the reaction as a transfer of a rigid cluster. In this method the two neutrons are treated as if they were an elementary particle of spin zero and mass two, and were present as such in the nucleus. With this picture, the calculation can be carried out in exactly the same way as a single-nucleon transfer such as (p, d) . In distorted-wave calculations of (p, d) , the form factor is usually taken to be the bound-state wave function of the neutron pair in a Woods-Saxon well. Such a cluster-transfer calculation was carried out using the wave function of a mass-two particle with quantum numbers $L=0$, $S=0$, and $J=0$. The calculations indicate that the general shape of the angular distributions are reproduced not nearly as well as with the two-particle form factor.

B. Transitions to the First 2^+ States

All six nuclei studied show a fairly well populated first excited state which is isolated from any other excited states that are populated. This state is either known or expected to be a $J^\pi = 2^+$ state.

Two-nucleon-transfer distorted-wave calculations were made for these states also. Again the wave functions for the initial and final states were assumed to be the very simplest. In particular, calculations were made assuming the pickup of a pair of neutrons from the same shell coupled to $J=2$. This was the $d_{5/2}$ shell for Ne, Mg, and Si and the $d_{3/2}$ shell for Ar and Ca. In the case of $^{32}\text{S}(p, t)^{30}\text{Si}$ (first 2^+), this is not possible, since there are two neutrons in the $2s_{1/2}$ shell and they must be coupled to zero. The ^{32}S ground state might be expected to contain admixtures of particles in the $d_{3/2}$, as well as the $s_{1/2}$ shell. Therefore, for this simple calculation of the $L=2$ shape, a pickup of one $s_{1/2}$ particle and one $d_{3/2}$ particle was assumed. The experimental distributions along with the results of the above calculations are shown in Fig. 7. The calculations are normalized to the first and the second peaks of the data.

C. Transitions to States in ^{18}Ne

Two-nucleon-transfer distorted-wave calculations were made for those transitions where the

TABLE IV. Energy levels of ^{26}Si . See text for explanation of notation.

This work		Other work		
Energy (MeV)	J^π	Energy (MeV)	J^π	References
		M.E. = -7.141 ± 0.011		
0.0*	0^+	0.00	0^+	36 41, $42_{J^\pi}^t$, 43, 44, 45, 46
$1.795^* \pm 0.011$	2^+	1.7959 ± 0.0002	2^+	41, 47_J , $42_{J^\pi}^t$, 44, 46, 47_E
$2.790^* \pm 0.012$	(2^+)	2.7835 ± 0.0004	2^+	41, 48, $42_{J^\pi}^t$, 43, 44, 45, 46, 47_E
$3.339^* \pm 0.019$		3.3325 ± 0.0003	(0)	41, 47_J , 43, 45, 47
		(3.770 ± 0.040)		43_E
		3.756 ± 0.002	(2^+)	$42_{J^\pi}^t$, 41, 47_E
		3.842 ± 0.002	3	48_J , 43, 47_E
$4.183^* \pm 0.011$	(2^+)	4.093 ± 0.003	(2)	41, 48_J , 43, 47_E
$4.457^* \pm 0.013$	$(2^+, 0^+)$	4.445 ± 0.003	(2^+)	41, $42_{J^\pi}^t$, 47_E
4.821 ± 0.013		4.805 ± 0.002		41, 47_E
5.229 ± 0.012				
5.562 ± 0.028				
5.960 ± 0.022				
6.381 ± 0.020				
6.786 ± 0.029				
7.150 ± 0.015				
7.476 ± 0.020				
7.695 ± 0.031				
7.902 ± 0.021				

experimental angular distributions were clear enough to indicate L transfer and for transitions to states where J^π assignments have been made by other workers. This nucleus has been studied previously using the (p, t) reaction by Falk *et al.*²³ and by L'Ecuyer *et al.*²⁹ The present results are shown in Fig. 8 along with the configuration of two picked-up neutrons assumed for purposes of calculation. This assumed configuration has little meaning, since it has been shown that shapes have only a small dependence on the configuration and are dominated by the L transfer. The calculations are arbitrarily normalized to make comparison of shape with data easier.

The experimental shape of the distribution to the state at 3.390 MeV is not well reproduced by the $L=4$ calculation which is shown with it in Fig. 8.

The $L=4$ assignment is best verified by comparison with the experimental distribution to the 3.323-MeV state in ^{22}Mg , which is most probably 4^+ by comparison with the level structure of its mirror nucleus ^{22}Ne . This is the basis for the tentative 4^+ assignment to this level at 3.390 MeV in ^{18}Ne . The $L=4$ fit by Falk *et al.*²³ is more convincing.

A triton group was observed at 3.614 MeV. Figure 8 shows both an $L=0$ and an $L=2$ calculation. The $L=0$ curve clearly fits much better at the forward angles. The existence of a 2^+ level at 3.6164 MeV has been established by Robertson *et al.*³⁰ along with a level at 3.5763 MeV which has been confirmed by Rolfs *et al.*³¹ This second state has been tentatively assigned a J^π value of 0^+ . The present level at 3.614 MeV may be the unresolved combination of these two levels as reported by

TABLE V. Energy levels of ^{30}S . See text for explanation of notation.

This work		Other work		
Energy (MeV)	J^π	Energy (MeV)	J^π	References
M.E. = -14.081 ± 0.012		M.E. = -14.063 ± 0.011		36
0.0*	0^+	0.0	0^+	41, 25, $42_{J^\pi}^t$, 43, 44, 45
2.239* ± 0.018	2^+	2.210 ± 0.018	2^+	41, 25_B , $42_{J^\pi}^t$, 43, 44, 45
3.438* ± 0.014	2^+	3.412 ± 0.025	2^+	41, 25_B , $42_{J^\pi}^t$, 43
3.707* ± 0.025	$((0^+))$	3.672 ± 0.023		41, 25_B , 43
		4.386 ± 0.031		25
		4.567 ± 0.030		25
		4.724 ± 0.020		25
5.207 ± 0.022		5.236 ± 0.015		25
5.306 ± 0.025				
		(5.381 ± 0.019)		25
5.426* ± 0.025				
		5.480 ± 0.015		25
		5.548 ± 0.024		25
		(5.657 ± 0.028)		25
		5.825 ± 0.019		25
5.897 ± 0.027				
		6.014 ± 0.012		25
(6.108 ± 0.029)		6.095 ± 0.010		25
(6.223 ± 0.030)		6.233 ± 0.010		25
6.415 ± 0.040				
6.861* ± 0.040				
7.185* ± 0.035				
7.570 ± 0.045				

*L'Ecuyer et al.*²⁹ in their (*p, t*) studies. If this is the case, the 0^+ member of the pair is by far the stronger.

The general features of the angular distribution to the level at 4.576 MeV are well reproduced by an $L=1$ calculation as shown in Fig. 8. But, a comparison with the $L=0$ ground-state-transition angular distribution shows that the maxima of the cross sections fall at the same angles. This triton group may correspond to the $0^+, 1^-$ doublet referred to by Adelberger and McDonald.³³

D. Transitions to States in ^{22}Mg

The state at 3.323 MeV in ^{22}Mg is tentatively assigned $J^\pi = 4^+$ although the shape is not well reproduced by the $L=4$ calculation shown in Fig. 9. This assignment is primarily based on a comparison with the known level structure of ^{22}Ne , the mirror nucleus to ^{22}Mg .

The levels at 4.417 and 5.057 MeV exhibit the features of an $L=2$ transition. Comparison with the transition to the known 2^+ level at 1.250 MeV verifies this (see Fig. 7). These two states are therefore tentatively assigned $J^\pi = 2^+$.

The state at 5.738 MeV has previously been very

tentatively assumed to be 0^+ (see Table III). An $L=0$ calculation is shown with the data in Fig. 9, but there is very little similarity. No attempt has been made to make a further assignment to this state.

The level at 6.061 MeV is undoubtedly the state observed by McDonald and Adelberger at 5.945 MeV.³⁵ The angular distribution to this state is quite well represented by the $L=0$ calculation shown in Fig. 9.

E. Transitions to States in ^{26}Si

The angular distribution to the state at 2.790 MeV in ^{26}Si is not complete enough to make a definite J^π assignment. It does exhibit some of the features of an $L=2$ distribution (see Fig. 10) and so a tentative 2^+ assignment is made. This is in agreement with the previous assignment (see Table IV).

The level at 3.339 MeV is very weakly excited. Its angular distribution is not consistent with the previous tentative $J=0$ assignment,⁴⁸ but no definite assignment can be made.

The shape of the distribution to the state at 4.183 MeV in ^{26}Si is quite well reproduced by an $L=2$

TABLE VI. Energy levels of ^{34}Ar . See text for explanation of notation.

This work		Other work		
Energy (MeV)	J^π	Energy (MeV)	J^π	References
M.E. = -18.370 ± 0.011		M.E. = -18.394 ± 0.013		36
0.0*	0^+	0.0	0^+	41, 43, 44, 49
2.094* ± 0.011	2^+	2.058 ± 0.035		41, 43, 44 _E
3.288* ± 0.014	2^+	3.30 ± 0.03		41 _E , 43
3.879 ± 0.015	0^+	3.90 ± 0.03		41
4.050 ± 0.014		4.05 ± 0.03		41
		4.15 ± 0.03		41
4.522 ± 0.014				
4.651 ± 0.014				
4.867 ± 0.014				
4.985 ± 0.014				
5.307* ± 0.013				
5.909 ± 0.012				
6.074 ± 0.011				
6.525 ± 0.009				
6.794* ± 0.011				
7.322 ± 0.006				
7.499 ± 0.004				
7.925* ± 0.005				

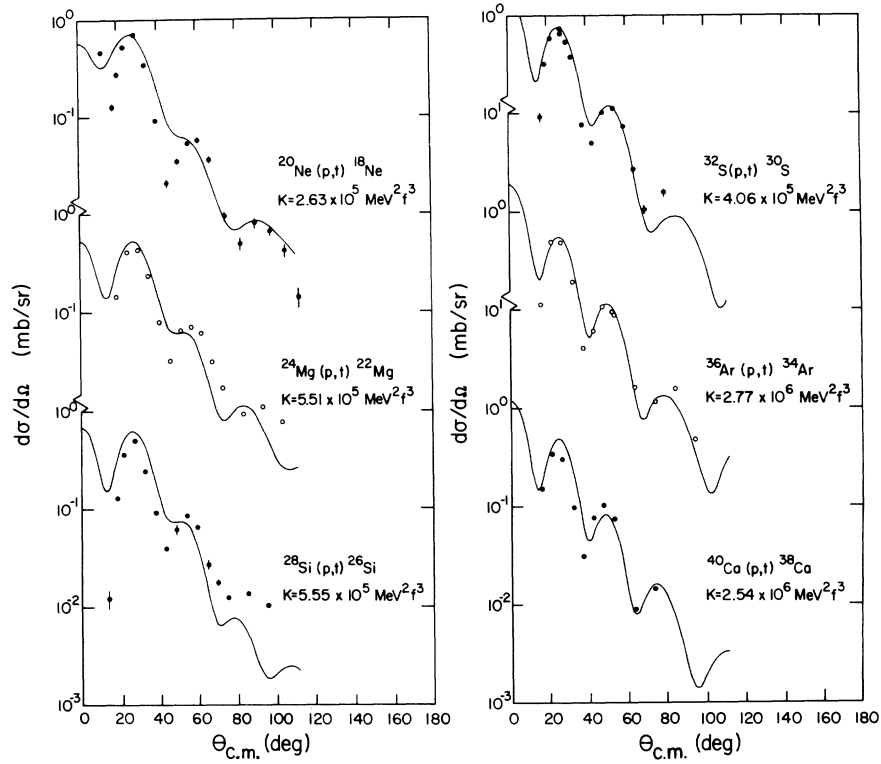


FIG. 6. 0^+ -to- 0^+ ground-state transitions. The distorted-wave calculations were multiplied by $K/5014$.

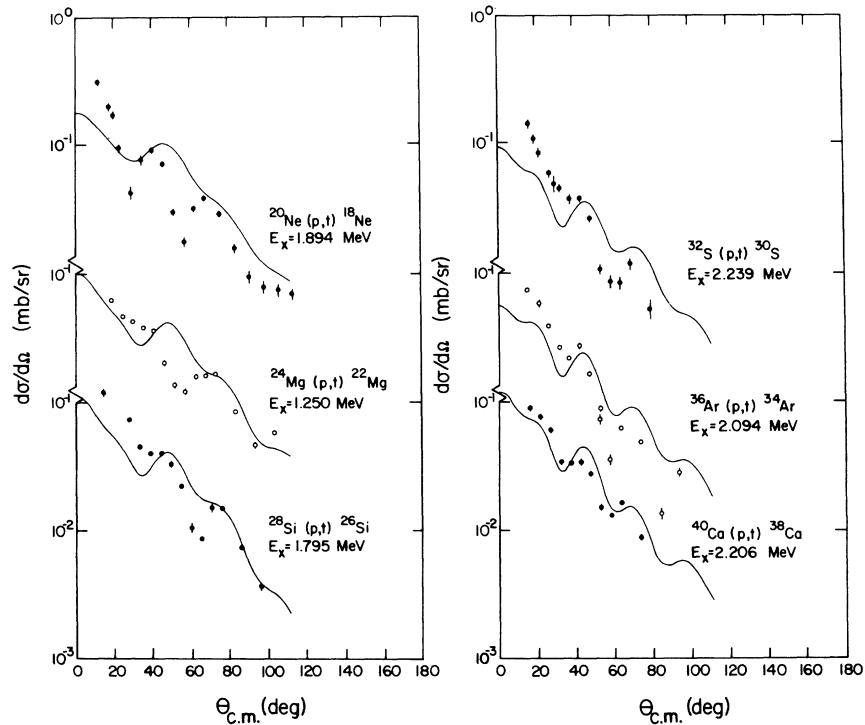
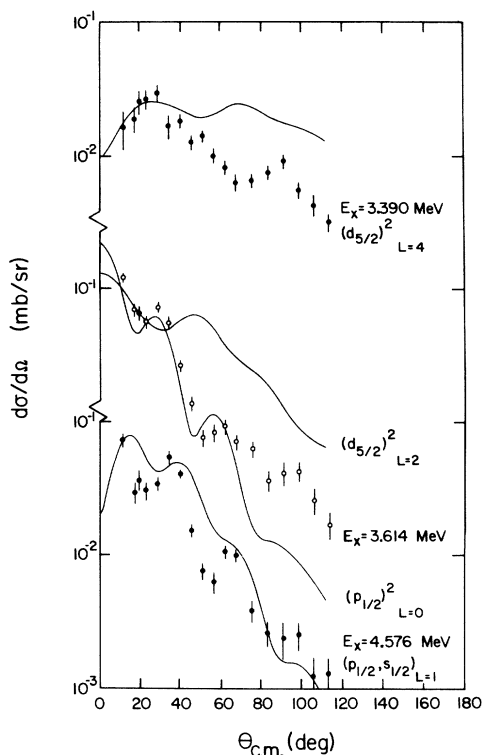


FIG. 7. Transition to the first 2^+ states.

FIG. 8. Transitions to states in ^{18}Ne .

calculation, but the state is only weakly excited and so only a tentative 2^+ assignment can be made.

Figure 10 shows both an $L=0$ and an $L=2$ calculation for the state at 4.457 MeV. The $L=0$ shape appears to give the better fit, but no definite assignment is made.

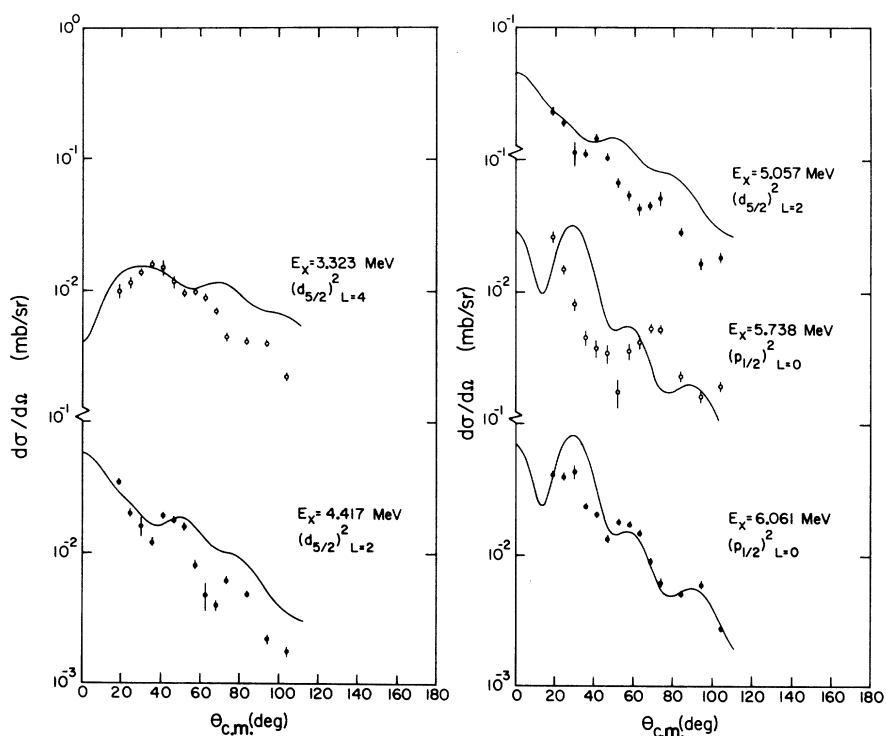
F. Transitions to States in ^{30}S

The shape of the angular distribution to the state at 3.438 MeV in ^{30}S is fairly well reproduced by an $L=2$ calculation as shown in Fig. 11. This state is therefore assigned a J^π value of 2^+ .

The state at 3.707 MeV is only weakly excited. The angles at which it was excited enough to extract a cross section correspond to the maxima of the $L=0$ ground-state-transition distribution to ^{30}S (see Fig. 6). Only a very tentative assignment of 0^+ can be made.

G. Transitions to States in ^{34}Ar

The reaction $^{36}\text{Ar}(p, t)^{34}\text{Ar}$ has not previously been reported. The angular distribution to the state at 3.288 MeV in ^{34}Ar exhibits very definite $L=2$ character. Comparison with the $L=2$ calculation shown in Fig. 12 and comparison with the distribution to the first 2^+ state in ^{34}Ar (see Fig. 7) both demonstrate this. A J^π value of 2^+ is there-

FIG. 9. Transitions to states in ^{22}Mg .

fore assigned to this state.

During many of the runs the levels at 3.879 and 4.050 MeV were not resolved. When it was possible to resolve them, it was obvious that the state at 3.879 MeV was more strongly excited by far.

Figure 12 shows the angular distribution is very well reproduced by this calculation, and so an 0^+ assignment can be made for the state at 3.879 MeV in ^{34}Ar .

The states at 5.909 and 6.074 MeV were also often not resolved, and the sum of the distributions to these two states is shown in Fig. 12. When these two states were resolved, it was not possi-

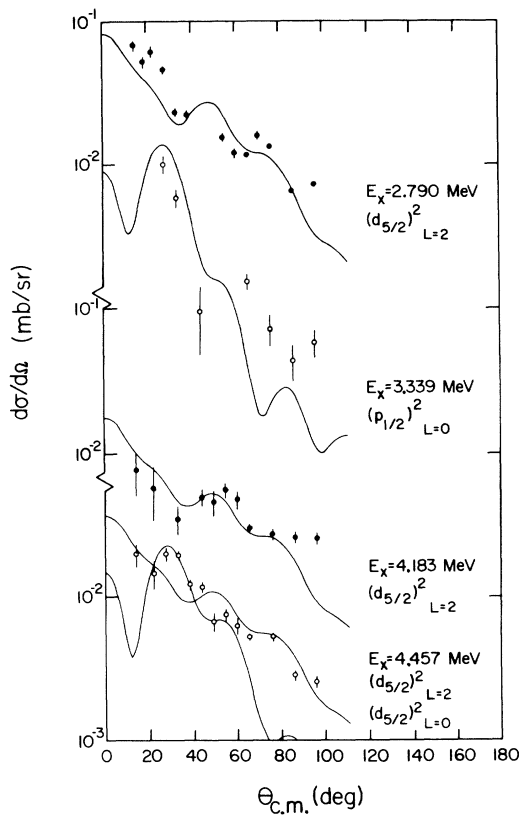
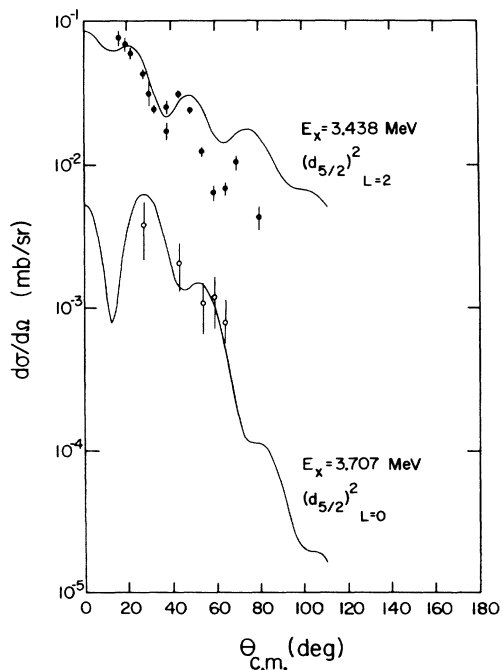
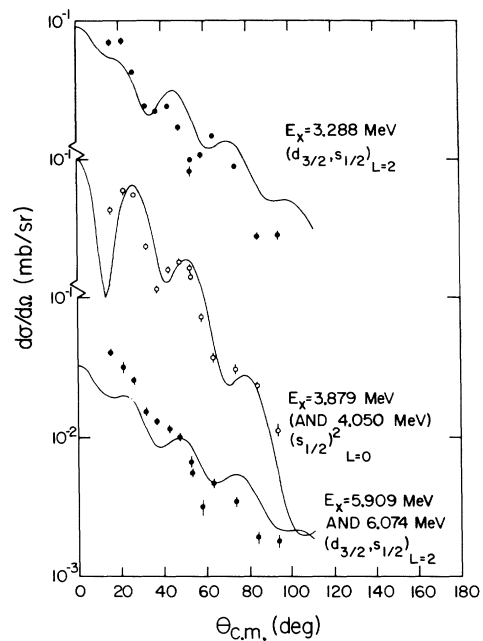
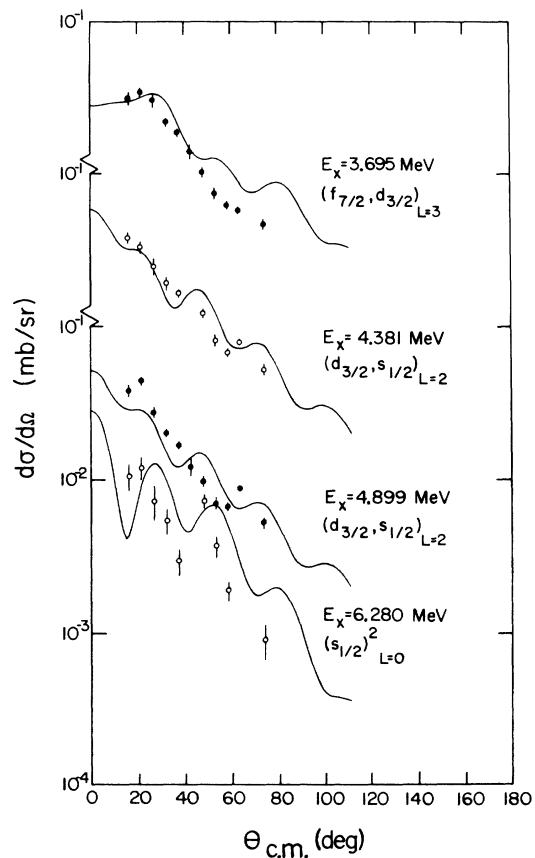
ble to say that one was much more strongly excited than the other. The total angular distribution does exhibit some $L=2$ character, and therefore possibly one or both states are 2^+ , but no definite assignment can be made.

H. Transitions to States in ^{38}Ca

A level in ^{38}Ca at 3.72 MeV has been reported by Hardy, Skyrme, and Towner⁵⁰ using the (p, t) reaction. This level was assigned a J^π value of 3^- . Recently Shapiro, Moss, and Denny⁵¹ have reported a 2^+ level at 3.69 MeV in ^{38}Ca seen by the

TABLE VII. Energy levels of ^{38}Ca . See text for explanation of notation.

This work		Other work		
Energy (MeV)	J^π	Energy (MeV)	J^π	References
M.E. = -22.081 ± 0.011		M.E. = -22.007 ± 0.021		50
		M.E. = -22.078 ± 0.040		42 ^t
		M.E. = -22.050 ± 0.025		51 ^t
0.0*	0^+	0.0	0^+	50, 42 ^t , 51 ^t _{Jπ}
$2.206^* \pm 0.005$	2^+	2.20 ± 0.03	2^+	50, 41 ^t _{EJπ} , 42 ^t
		3.06 ± 0.05	0^+	50
		3.69 ± 0.03	2^+	50
$3.695^* \pm 0.005$		3.72 ± 0.03	3^-	42, 51 ^t _{EJπ}
4.191 ± 0.005				
$4.381^* \pm 0.005$	(2^+)	4.391 ± 0.040	2^+	52, 42 ^t _{EJπ}
$4.748^* \pm 0.005$				
$4.899^* \pm 0.005$	(2^+)	4.886 ± 0.040	2^+	50, 42 ^t _{EJπ} , 51 ^t
$5.159^* \pm 0.007$				
		5.219 ± 0.040		42 ^t
$5.264^* \pm 0.005$				
5.427 ± 0.006				
5.598 ± 0.007				
5.698 ± 0.010				
$5.810^* \pm 0.005$				
6.136 ± 0.006				
$6.280^* \pm 0.008$	(0^+)			
6.598 ± 0.007				
6.702 ± 0.010				
6.768 ± 0.015				
6.801 ± 0.012				
(7.208 ± 0.015)				
7.800 ± 0.012				
8.595 ± 0.010				

FIG. 10. Transitions to states in ^{26}Si .FIG. 11. Transitions to states in ^{30}S .FIG. 12. Transitions to states in ^{34}Ar .FIG. 13. Transitions to states in ^{38}Ca .

$(^3\text{He}, n)$ reaction. In the present experiment, a level at 3.695 MeV was observed. The angular distribution to this state is shown in Fig. 13. An $L=3$ distorted-wave calculation is shown along with it, but an $L=2$ shape fits it nearly as well. If the two states previously reported are actually the same, the present experiment does not resolve the spin discrepancy. The 0^+ state at 3.06 MeV reported by Shapiro, Moss, and Denny⁵¹ was not observed at all in the present experiment.

The angular distribution to the states at 4.381 and 4.899 MeV both resemble an $L=2$ shape (see Fig. 13), but the distributions are not complete enough to make a definite assignment.

The level at 6.280 MeV in ^{38}Ca was only weakly excited by the (p, t) reaction. The distribution to this state resembles an $L=0$ transition as shown in Fig. 13. The transition is too weak and the distribution is not complete enough to make any more than a tentative 0^+ assignment to this level.

VI. SUMMARY

In this work it has been found that the (p, t) reaction is useful as a method of studying the energy levels of nuclei. It is practically unique along with $(^3\text{He}, n)$ for studying nuclei two nucleons away from stability. The energies of the tritons from the (p, t) reaction have been used to locate levels in the nuclei ^{18}Ne , ^{22}Mg , ^{26}Si , ^{30}S , ^{34}Ar , and ^{38}Ca .

The two-nucleon-transfer theory of Glendenning¹¹ and the distorted-wave method give shapes which

fairly well reproduce the experimental angular distributions. The shapes were found to be dominantly characterized by the L transfer, and this quality was used to make spin-parity assignments to some of the levels observed. The magnitudes of the predicted cross sections were found to be influenced very greatly by the optical-model parameters, the bound-state parameters, and, most importantly, the presence of admixtures in the shell-model wave functions of the nuclear states. It is concluded that these strong dependences make the prediction of magnitudes of cross sections for the (p, t) reaction extremely useful for studies of more detailed shell-model wave functions. The detailed calculations using parentage factors from realistic shell-model wave functions are presently being carried out as a part of a larger program concerning the shell model of the $2s1d$ shell. These results will be reported separately.⁵²

ACKNOWLEDGMENTS

The author is indebted to Dr. W. Benenson for suggesting these experiments as a thesis project. The assistance of I. D. Proctor and Dr. P. J. Lo-card in taking the data is gratefully acknowledged. We would like to thank Professor R. M. Drisko for making a copy of the FORTRAN-IV version of JULIE available. We would also like to thank Dr. W. Gerace for making a copy of the code TWOFRM available to the Michigan State University Cyclotron Laboratory.

*Work supported by the National Science Foundation.

†Ph.D. thesis; present address: Ripon College, Ripon, Wisconsin.

¹J. Cerny, R. H. Pehl, and G. T. Garvey, *Phys. Letters* **12**, 234 (1964).

²D. G. Fleming, J. Cerny, C. Maples, and N. Glendenning, *Phys.* **166**, 1012 (1968).

³G. T. Garvey, J. Cerny, and R. H. Pehl, *Phys. Rev. Letters* **12**, 726 (1964).

⁴G. Bassani, N. M. Hintz, and C. D. Kavaloski, *Phys. Rev.* **136**, B1006 (1964).

⁵G. Bassani, N. M. Hintz, C. D. Kavaloski, J. R. Maxwell, and G. M. Reynolds, *Phys. Rev.* **139**, B830 (1965).

⁶B. F. Bayman and N. M. Hintz, *Phys. Rev.* **172**, 1113 (1968).

⁷J. R. Maxwell, G. M. Reynolds, and N. M. Hintz, *Phys. Rev.* **151**, 1000 (1966).

⁸G. M. Reynolds, J. R. Maxwell, and N. M. Hintz, *Phys. Rev.* **153**, 1283 (1967).

⁹J. M. Blatt, G. H. Derrick, and J. N. Lyness, *Phys. Rev. Letters* **8**, 323 (1962).

¹⁰G. R. Satchler, *Nucl. Phys.* **55**, 1 (1964).

¹¹N. K. Glendenning, *Phys. Rev.* **137**, B102 (1965).

¹²D. M. Drisko and F. Rybicki, *Phys. Rev. Letters* **16**, 275 (1966).

¹³R. L. Jaffe and W. J. Gerace, Princeton University Report No. PUC-937-329, July 1968 (unpublished).

¹⁴R. H. Bassel, R. M. Drisko, and G. R. Satchler, Oak Ridge National Laboratory Report No. ORNL-3240, 1962 (unpublished), and Oak Ridge National Laboratory Memorandum to the Users of the Code JULIE, 1966 (unpublished).

¹⁵M. P. Fricke and G. R. Satchler, *Phys. Rev.* **139**, B567 (1965).

¹⁶E. R. Flynn, D. D. Armstrong, J. G. Beery, and A. G. Blair, to be published.

¹⁷G. MacKenzie, E. Kashy, M. M. Gordon, and H. G. Blosser, *IEEE Trans. Nucl. Sci.* **14**, 450 (1967).

¹⁸C. F. Williamson, J. Boujot, and J. Picard, Centre d'Etudes Nucléaire de Saclay Report No. CEA-R3042, 1966 (unpublished).

¹⁹R. L. Kozub, Ph.D. thesis, Michigan State University, 1967 (unpublished).

²⁰F. S. Goulding, D. A. Landis, J. Cerny, and R. H. Pehl, *Nucl. Instr. Methods* **31**, 1 (1964).

²¹D. Bayer and W. Benenson, *Bull. Am. Phys. Soc.* **14**, 1243 (1969).

²²J. H. E. Mattauch, W. Thiele, and A. H. Wapstra, *Nucl. Phys.* **67**, 1 (1965).

²³W. R. Falk, R. J. Kidney, P. Kulisic, and G. K. Tandon, *Nucl. Phys.* **A157**, 241 (1970).

- ²⁴D. K. Olsen and R. E. Brown, John H. Williams Laboratory of Nuclear Physics, University of Minnesota, Report No. COO-1265-67, 1968 (unpublished).
- ²⁵M. H. Shapiro, University of Rochester, private communication.
- ²⁶J. H. Towle and G. J. Wall, Nucl. Phys. **A118**, 500 (1968).
- ²⁷M. Krick and G. J. F. Legge, Nucl. Phys. **89**, 63 (1966).
- ²⁸N. H. Gale, J. B. Garg, and K. Ramavataram, Nucl. Phys. **22**, 500 (1961).
- ²⁹J. L'Ecuyer, R. D. Gill, K. Ramavataram, N. S. Chant, and D. G. Montague, Phys. Rev. C **2**, 116 (1970).
- ³⁰B. C. Robertson, R. A. I. Bell, J. L'Ecuyer, R. X. Gill, and H. J. Rose, Nucl. Phys. **A126**, 431 (1969).
- ³¹C. Rolfs, W. Trost, F. Riess, R. Kramer, and E. Kuhlmann, Nucl. Phys. **A137**, 481 (1969).
- ³²M. H. Shapiro, A. Adams, C. Moss, and W. M. Denny, Nucl. Phys. **A144**, 17 (1970).
- ³³E. G. Adelberger and A. B. McDonald, to be published.
- ³⁴J. Cerny, S. W. Cosper, G. W. Butler, R. H. Pehl, F. S. Goulding, D. A. Landis, and C. Détraz, Phys. Rev. Letters **16**, 469 (1966).
- ³⁵A. B. McDonald and E. G. Adelberger, Nucl. Phys. **A144**, 593 (1970).
- ³⁶P. M. Endt and C. Van der Leun, Nucl. Phys. **A105**, 1 (1967).
- ³⁷N. K. Ganguly, A. A. Rush, E. J. Burge, and D. A. Smith, Rutherford Laboratory Report No. RHEL/R 156, 1967 (unpublished); and Bull. Am. Phys. Soc. **12**, 664 (1967).
- ³⁸J. W. Olness, A. R. Poletti, and E. K. Warburton, Phys. Rev. **161**, 1131 (1967).
- ³⁹R. Benenson and I. J. Taylor, Bull. Am. Phys. Soc. **11**, 737 (1966).
- ⁴⁰J. Cerny, S. W. Cosper, G. W. Butler, R. H. Pehl, F. S. Goulding, D. A. Landis, and C. Détraz, Phys. Rev. Letters **16**, 469 (1966).
- ⁴¹M. Hagen, K. H. Maier, and R. Michaelsen, Phys. Letters **26B**, 432 (1968).
- ⁴²W. G. Davies, J. C. Hardy, D. J. Skyrme, D. G. Montague, K. Ramavataram, and T. A. Hodges, Rutherford Laboratory Report No. RHEL/R 156, 1967 (unpublished).
- ⁴³W. R. McMurray, P. Van der Merwe, and I. J. Van Heerden, Nucl. Phys. **A92**, 401 (1967).
- ⁴⁴R. G. Miller and R. W. Kavanagh, Nucl. Phys. **A94**, 261 (1967).
- ⁴⁵W. R. McMurray, P. Van der Merwe, and I. J. Van Heerden, Phys. Letters **18**, 319 (1965).
- ⁴⁶F. Ajzenberg-Selove and K. L. Dunning, Phys. Rev. **119**, 1681 (1960).
- ⁴⁷R. A. I. Bell, J. L'Ecuyer, R. B. Gill, B. C. Robertson, I. S. Towner, and H. J. Rose, Nucl. Phys. **A133**, 337 (1969).
- ⁴⁸C. Rolfs and W. Trost, Nucl. Phys. **A122**, 633 (1968).
- ⁴⁹R. G. Miller and R. W. Kavanagh, Phys. Letters **22**, 461 (1966).
- ⁵⁰J. C. Hardy, D. J. Skyrme, and I. S. Towner, Phys. Letters **23**, 487 (1966).
- ⁵¹M. H. Shapiro, C. Moss, and W. M. Denny, Nucl. Phys. **A128**, 73 (1969).
- ⁵²B. H. Wildenthal and W. Benenson, to be published.

Levels of ⁵⁹Co Populated in Compound-Nuclear Reactions*

A. J. Kennedy, J. C. Pacer, A. Sprinzak, J. Wiley, and N. T. Porile

Department of Chemistry, Purdue University, Lafayette, Indiana 47907

(Received 23 August 1971)

Highly excited levels of ⁵⁹Co have been populated by the ⁵⁹Co(*p*, *p'*) and ⁶²Ni(*p*, *α*) reactions induced by 14.0-MeV protons and by the ⁵⁶Fe(*α*, *p*) and ⁵⁹Co(*α*, *α'*) reactions induced by 16.5-MeV *α* particles. Energy spectra were measured over the 30–150° angular interval and the results compared with the spin- and isospin-dependent statistical theory. The (*p*, *α*), (*α*, *α'*), and (*α*, *p*) reaction spectra could all be fitted with the same level-density parameter and pairing energy of ⁵⁹Co: *a* = 7.5 MeV⁻¹ and *δ* = 1.29 MeV. In order to obtain agreement with these same parameters for the (*p*, *p'*) reaction spectrum it was necessary to invoke a 30–40% contribution from a pre-equilibrium emission process. The sensitivity of the results of the various parameters of the theory is explored.

I. INTRODUCTION

Compound-nuclear reactions populate highly excited levels of nuclei and offer a unique method for studying various properties of these levels. Information about the density of highly excited levels has been obtained from the analysis of the energy spectra of evaporated particles,^{1,2} from ex-

citation functions of isolated levels,³ and from integral cross sections and excitation functions.^{4,5} This subject has been summarized from various viewpoints in several recent reviews^{6–8} which indicate that the properties of interest, e.g., the level-density parameter, depend to some extent on the type of measurement as well as the particular parametrization of the statistical theory used